Nanoscale Advances

ROYAL SOCIETY OF CHEMISTRY

COMMUNICATION

View Article Online
View Journal | View Issue

Cite this: *Nanoscale Adv.*, 2025, **7**, 1009

Received 7th October 2024
Accepted 23rd December 2024

DOI: 10.1039/d4na00835a

rsc.li/nanoscale-advances

Fusion of polymer-coated liposomes and centrifugally spun microfibers as hybrid materials to enhance sustained release†

Ahmed M. Agiba, [a] Luis Gerardo Rodríguez Huerta, [a] Nicolás A. Ulloa-Castillo, [b] Francisco J. Sierra-Valdez, [a] Saeed Beigi-Boroujeni, [a] Omar Lozano *[cd] and Alan Aguirre-Soto *[ab]

Liposomes are employed for the delivery of molecular cargo in several classes of systems. For instance, the embedding of loaded liposomes in polymeric fibrous scaffolds has enabled the creation of hybrid materials that mimic biological membranes. Liposomes with unmodified surfaces have been predominantly integrated into fibers, which leads to instabilities due to interfacial incompatibility. In addition, electrospinning has been almost exclusively employed for fiber fabrication, which limits the potential for scale-up production. Here, we present the fabrication of hybrid biomimetic materials by fusing polymer-coated liposomes to force-spun microfibers to increase the stability of the hybrid materials and enhance the sustained release of the cargo. L-α-Phosphatidylcholine liposomes were coated with chitosan or polyethylene glycol (PEG). The nano-differential scanning calorimetry results confirm that polymer coating does not affect the phase transition temperature (T_m) of the liposomes, where only the model drug, quercetin, reduced T_m. Centrifugal spinning was employed to fabricate hydrophobic polycaprolactone (PCL) microfibers at various polymer concentrations and using various solvents and spinning parameters to increase the yield at the lowest fiber diameter. The highest microfiber production rate obtained occurred at a 20% (w/v) PCL concentration in 50 : 50 (v/v) chloroform and methanol solution with an average fiber diameter of 584.85 ± 26.30 nm. The non-chemical fusion of the polymer-coated liposomes and the fibrous scaffolds was promoted by immersion at $T > T_m$, under ultrasonication. We hypothesize that the fusion is driven by hydrophobic interactions between the liposomes and the fibers, which merge the materials through the lipid bilayer. The fused hybrid material solved the burst release problem observed when adhering plain liposomes to nanofibers. Both PEG and chitosan yielded a sustained release, where the release rate with the former was faster. These results demonstrate that the fusion of polymer-coated liposomes and microfibers enables more effective blending of the loaded carriers into the polymer microfibers. Ultimately, the fused liposome/microfiber hybrids are stable matrices and enhance the sustained release of molecular cargo.

1 Introduction

Over the last four decades, the use of liposomes has greatly expanded into ever more complex molecular delivery systems.[1,2] A wide range of carrier ensembles have utilized vesicles of various chemistries, particle sizes, charges, and surface functionalization. However, their implementation has generally been challenged by the low stability of the self-assembled amphiphilic membranes and the limited resilience of their structure throughout the processes required for their incorporation into practical formulations. Despite the successful implementation of a few liposomal suspensions, several opportunities remain for the development of next-generation solutions to address the hurdles that hinder a broader translation of these versatile materials.

On the other hand, polymeric fibers with nano- and microscale size features have been used as delivery systems on their own by loading molecular cargo into their porous structure, Fig. 1a.[3] Their tunable porosity, high surface-to-volume ratio, and release rates make them interesting alternatives for molecular release. Three fiber production techniques are available, namely, electrospinning, centrifugal, and electrocentrifugal spinning.[4] Electrospinning is the oldest and most widely used technique, based on the electrostatic pulling of polymers out from solution. Centrifugal spinning enables the high-throughput production of polymeric fibrous scaffolds or mats through the application of centrifugal forces, as depicted in Fig. 1b. The fiber production rates with centrifugal spinning exceed 1 g min^{-1}, which is significantly higher than that of equivalent electrospinning devices, 0.1 g min^{-1}.[5] Moreover, centrifugal spinning enables the production of high-quality

[a]School of Engineering and Sciences, Tecnologico de Monterrey, Monterrey 64849, Nuevo León, Mexico. E-mail: alan.aguirre@tec.mx

[b]Center for Innovation in Digital Technologies, School of Engineering and Sciences, Tecnologico de Monterrey, Monterrey 64849, Nuevo León, Mexico

[c]Institute for Obesity Research, Tecnologico de Monterrey, Monterrey 64849, Nuevo León, Mexico. E-mail: omar.lozano@tec.mx

[d]School of Medicine and Health Sciences, Tecnologico de Monterrey, Monterrey 64849, Nuevo León, Mexico

† Electronic supplementary information (ESI) available. See DOI: https://doi.org/10.1039/d4na00835a

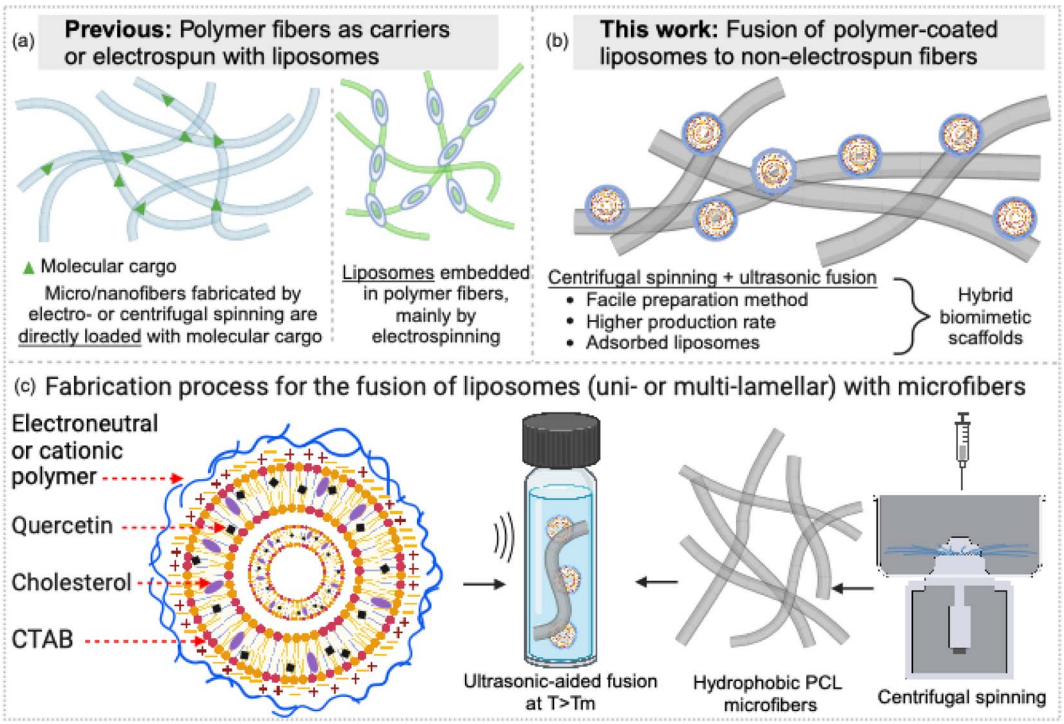

Fig. 1 Conceptual framework for the fusion of polymer-coated liposomes and microfibers. (a) Previous work on the direct loading of molecular cargo into fibrous scaffolds and the fabrication of fibers mainly by electrospinning. (b) Schematic representation of polymer-coated liposomes fused to polycaprolactone (PCL) microfibers. (c) Scalable fabrication process for hybrid materials based on centrifugal spinning and fiber immersion.

fibrous mats from either polymeric solutions or melts, as well as from conductive and non-conductive polymers.[6,7] The surface morphology and the mechanical properties of the obtained fibers are determined by the polymer viscoelasticity, solvent surface tension, solvent evaporation rate, spinneret angular velocity and aspect ratio, spinneret orifice distance to the collector, orifice radius and orientation, and solvent fill volume.[4,5] Fibers produced by electrospinning or centrifugal spinning have both been reported to be directly loaded with molecular cargo during and after the spinning process. Utilizing the porosity and swelling of the polymer materials, molecules have been embedded within the fibers for the subsequent release. Nevertheless, the release kinetics profiles obtained with these approaches are generally limited to relatively short dose periods for a small set of molecular cargo chemistries.

The loading of liposomes into fibrous scaffolds has been exploited to combine the benefits of both the liposomal and polymer carriers (Fig. 1a).[8] Most reports describe the combination of plain liposomes and electrospinning, where the lipids are dissolved along with the polymers before the application of the electromagnetic field. However, liposome loading into fibers is challenged by aggregation, degradation, hydrolysis, and phospholipid oxidation.[9–11] These challenges have been tackled to some extent through optimization of the lipid-to-polymer ratio and the spinning parameters. In contrast, only one study was found on the use of centrifugal spinning for fiber fabrication and subsequent adhesion of liposomes for the release of molecular cargo. Rampichová *et al.* prepared fibrous scaffolds of polycaprolactone (PCL) by centrifugal spinning with adhered liposomes.[12] The problem is that the authors documented an uncontrolled burst release (~15 min) of the incorporated molecule. Further work was suggested to fabricate more stable materials that can sustain the release of cargo at a constant rate for longer.

In this work, we present the fusion of polymer-coated liposomes with polymeric fibrous scaffolds (Fig. 1b) through a scalable procedure that merges centrifugal spinning and fiber immersion (Fig. 1c). We propose that the fusion of the polymer-coated liposomes and the microfibers is driven by hydrophobic forces during immersion of both materials under ultrasound at a temperature over the phase transition temperature of the liposomes. No reports were found on the combination of fibers fabricated by centrifugal spinning with polymer-coated liposomes. Liposomes conformed by L-α-phosphatidylcholine (PC) vesicles and cholesterol are loaded with quercetin (QR) as a model hydrophobic drug and cetyltrimethylammonium bromide (CTAB) as a bioenhancer. Loaded liposomes were coated with chitosan or polyethylene glycol. The polymer-coated liposomes are intended to stabilize the lipid bilayer during fusion with hydrophobic PCL microfibers. The hybrid materials were characterized, and their drug release kinetics were compared against plain and coated liposomes. QR is a naturally occurring antioxidant flavonoid with a variety of biological activities, including anticancer, anti-inflammatory, cardiovascular disease prevention, and hepatoprotective activity.[13] However, the therapeutic use of QR is limited due to its poor aqueous solubility, chemical instability, and low bioavailability,

which greatly restricts its therapeutic potential as a functional active ingredient.[14] Encapsulating phytochemicals in liposomes remains cumbersome.[15] Therefore, the hybrid materials presented here are proposed as a framework for the encapsulation and subsequent sustained release of challenging molecular cargo *via* a scalable fabrication process.

2 Experimental section

Quercetin (>95% HPLC), L-α-PC (≥95% phosphatides, soybean, powder), cholesterol (>98%, ovine wool), cetyltrimethylammonium bromide (CTAB), 190–310 kDa chitosan, polyethylene glycol (PEG)-4000, 80 kDa polyvinyl alcohol (PVA), 80 kDa polycaprolactone (PCL), sodium acetate trihydrate, glacial acetic acid, sodium hydroxide, dimethylformamide (DMF), tetrahydrofuran (THF), dimethyl sulfoxide (DMSO), trifluoroacetic acid (TFA), HPLC-grade chloroform and HPLC-grade methanol were supplied by Sigma-Aldrich Corp., USA, and used as received. Spectra/Por® 3 dialysis tubing was purchased from Spectrum Laboratories, Inc., USA.

2.1 Preparation of loaded liposomes

Liposomes were prepared by the thin-film hydration method followed by sonication.[16] A total weight of 900 mg of L-α-PC and cholesterol was dissolved in 15 mL of a 2 : 1 (v/v) mixture of chloroform and methanol in a 500 mL rotary evaporator round-bottom flask containing 150 mg of QR (Table S1 and Fig. S1†). The organic phase was slowly removed in a rotary evaporator (Witeg Labortechnik GmbH, Germany) at 40 °C and 150 rpm, and a thin lipid film was formed on the flask inner surface. The dry lipid film was hydrated with 15 mL of purified water at 40 °C containing the CTAB bioenhancer for 45 minutes. The resulting liposomes were sequentially placed in an ultrasonic bath (Branson CPX-952-238R, Branson Ultrasonics Corp., USA) for 2 hours and then stored in 30 mL amber-colored glass bottles sealed with parafilm in a refrigerator at 2–8 °C for overnight maturation.

2.2 Polymer coating of loaded liposomes

All formulations contained 10 mg of quercetin, 38 mg of phospholipid, 19 mg of cholesterol and 5.7 mg of CTAB. Chitosan and PEG were used at 0.5 and 40 mg loadings. Liposomes were mixed with a 0.05% (w/v) chitosan solution in 100 mM acetate buffer solution (pH 4.4) or a 4% (w/v) aqueous solution of PEG-4000 (Table S1†), in equal volumes (1 : 1), and mechanically stirred at 10 000 rpm for 30 minutes.[17] The coated liposomes were then placed in an ultrasonic bath for 5 minutes and then stored in 30 mL amber-colored glass bottles sealed with parafilm in the refrigerator at 2–8 °C until further use.

2.3 Fabrication of polycaprolactone (PCL) fibers

A PCL solution (20%, w/v) was prepared in a 50 : 50 (v/v) mixture of chloroform and methanol stirred for 2 hours (Table S1†). Solutions were stored at room temperature until further use. Two milliliters of the PCL solution were injected into a dual-orifice spinneret of a Forcespinning® FiberLab L1000 (FibeRio Technology Corporation, USA) instrument equipped with two disposable needles (BD Precision Glide, 30 G × 1/2) and rotated at 9000 rpm for 50 seconds. The temperature and relative humidity were set to be 34 °C and 37–41%, respectively.

2.4 Fusion of polymer-coated liposomes and microfibers

The PCL microfibers were immersed in the liposomal suspensions and sonicated for 5 minutes. The hybrid fibers were washed several times with purified water to remove non-loaded liposomes and oven-dried (Shel Lab, USA) at 35 °C for 30 minutes.

2.5 Dynamic light scattering (DLS) and viscosity of liposomal suspensions

The particle size, polydispersity index (PDI), and zeta potential of freshly prepared coated liposomes were measured using a Zetasizer Nano ZS (Malvern Instruments Ltd, Worcestershire, UK). A 250 μL aliquot of the liposomal suspension was diluted with deionized water at a 1 : 20 (v/v) ratio and measured in a zeta cell. The viscosity was measured using a digital viscometer (Brookfield DV-II + PRO, Brookfield Engineering Laboratories, Inc., USA) using spindle 61 (LV1) at 60 rpm and 37 °C.

2.6 Entrapment efficiency and drug loading capacity

The free drug was separated from the liposomal suspension by centrifugation (Sorvall, ST 40R centrifuge, Thermo Fisher Scientific, USA) at 13 000 rpm for 30 minutes. The supernatant was filtered through a 0.22 μm pore-size nylon syringe filter (Thermo Fisher Scientific, USA) and analyzed for the free drug, in which the concentration of QR was determined using a UV-Vis spectrophotometer (Cary 7000, Agilent Technologies, Santa Clara, CA, USA). The calibration is detailed in Table S2 and Fig. S2† for the calculation of entrapment efficiency (EE%) and drug loading capacity (LC%).

2.7 Release kinetics studies

The QR release from liposomes was carried out using the Spectra/Por® 3 dialysis tubing (Spectrum Laboratories, Inc., USA) with a molecular weight cutoff (MWCO) of 3.5 kDa, a pore size of <10 nm, and a 10 cm length with a membrane diameter of 11.5 mm.[18] Release studies were performed in phosphate-buffered saline (PBS) at pH 7.4, where 2 mL (equivalent to 20 mg QR) of each liposomal formulation were transferred to a dialysis tube, the upper end of which was tied off, and then immersed into 250 mL glass beakers containing 100 mL of PBS at a pH of 7.4 and 0.1% (v/v) PEG-400 as a solubilizer. Beakers were placed on magnetic stirrers (IKA, C-MAG HS 7 digital, Staufen, Germany) at a temperature of 37 ± 0.5 °C and a stirring speed of 100 rpm. An aliquot (4 mL) was withdrawn at specific time intervals and replaced with an equal amount of fresh PBS. For the fused liposome/microfibers materials, samples were placed in PBS at pH 7.2, at a rotation speed of 100 rpm and a temperature of 37 °C.[19] All aliquots were filtered through a 0.22 μm pore-size nylon syringe filter (Thermo Fisher

Scientific, USA), and the amount of QR released was determined using a UV-Vis spectrophotometer.[20] The data obtained from drug release studies were evaluated using the following release models: zero-order, first-order, the Higuchi square root, the Hixson–Crowell cube root, and Korsmeyer–Peppas.

2.8 Nano-differential scanning calorimetry (DSC) of liposomal suspensions

Heat capacity profiles were recorded with a nanocalorimeter (Nano DSC, TA Instruments, Delaware, USA) at a constant scan rate of 1 °C min^{-1}, a constant pressure of 3 atm, and a cooling mode from 70 to −10 °C. Samples were degassed at low pressure (635 mmHg) for 10 min at 25 °C before loading into the DSC capillaries. Thermograms were analyzed with the NanoAnalyze software (v3.12.0; TA Instruments, Delaware, USA) provided with the instrument.[21]

2.9 Scanning electron microscopy (SEM)

The surface morphology of the materials was studied using a scanning electron microscope (SEM, ZEISS EVO® MA 25, Ostalbkreis, Baden-Württemberg, Germany). Samples were coated with a thin layer of gold. ImageJ software was used to calculate the average diameter of the prepared forcespun microfibers from high-resolution SEM images.[22]

2.10 Fourier-transform infrared spectroscopy (FT-IR)

An FT-IR spectrophotometer (PerkinElmer Universal ATR Sampling Accessory Frontier, Waltham, MA, USA) was used in a scanning range of 400–4000 cm^{-1}.[22]

2.11 Thermal gravimetric analysis (TGA)

Thermal gravimetric analysis (TGA, Pyris 8000, PerkinElmer, Delaware, USA) was performed to determine the mass loss of the materials. The heating rate was set at 10 °C min^{-1} under a nitrogen atmosphere, with temperatures ranging from 20 °C to 750 °C.[22]

2.12 Statistical analysis

Data are expressed as mean ± standard deviation (SD) for physicochemical characterization and drug release studies. All statistical analyses were made using ANOVA, followed by a Tukey–Kramer test for multiple comparisons using GraphPad Instat® software.

3 Results and discussion

3.1 Preparation and characterization of liposomes

As shown in Table S3,† the size of the chitosan and PEG coated liposomes was 552.62 ± 25.12 nm and 469.08 ± 48.75 nm, respectively. The PDIs were 0.48 ± 0.06 and 0.55 ± 0.06, respectively, which are common for unextruded liposomes.[23,24] The zeta potentials were 30.18 ± 1.36 and 14.57 ± 0.95 mV, respectively. The chitosan-coated liposomes had a higher zeta potential than those with PEG coating due to the positive charge from the chitosan. In general, the higher physical stability and positive charge of coated liposomes could be attributed to increased charge density and a thicker outer film layer, which could decrease liposome coalescence and aggregation during storage.[25] Furthermore, the dynamic viscosity of the polymer-coated liposomes was 11.94 ± 3.79 cP with chitosan and 12.79 ± 6.79 cP with PEG (Table S3†).

An EE% of 96.82 ± 0.007% was obtained with the chitosan-coated liposomes. In contrast, 96.39 ± 0.002% of the quercetin was encapsulated with the PEG-coated liposomes. The LC% was 9.381 ± 0.01% and 8.794 ± 0.003% for the chitosan and PEG coatings, as shown in Fig. S3a and Table S3.† Despite the high drug entrapment efficiency, the loading capacity of liposomes was limited because it depends on the drug/lipid ratio and the available space in the lipid bilayer.[26]

The key challenge with liposome stability is liposome aggregation, a sign of low physical stability during storage. Following 3 months of storage at 2–8 °C, the coated liposomes showed good colloidal stability, as indicated by negligible variations ($p < 0.05$) in zeta potential, PDI, and particle size (Table S3†). This is explained by the high concentration of cholesterol in liposomes, which improves the integrity of the liposomal membrane and serves as a stabilizer.

To further evaluate the stability of the lipid bilayer as a function of the molecular cargo and polymer coating, thermograms were obtained for each liposomal suspension as shown in Fig. 2. L-α-PC exhibited a wide and bimodal gel-liquid thermogram. However, the addition of cholesterol to the liposomes (LP) caused a slight shift to higher temperatures, indicating increased lateral cohesion and stability of the lipid bilayer, as in biological membranes.[27] Cholesterol preserved the bimodal phase transition, suggesting the absence of lipid remodeling. In contrast, when QR was anchored into the lipid bilayer, it weakened lipid-to-lipid interactions, as evidenced by the gel-liquid phase transition shifting to lower temperatures.[28] Furthermore, the unimodal phase transition peak demonstrated that QR caused a homogeneous distribution of lipid species. Moreover, PC/Chol/QR/CTAB showed that the CTAB

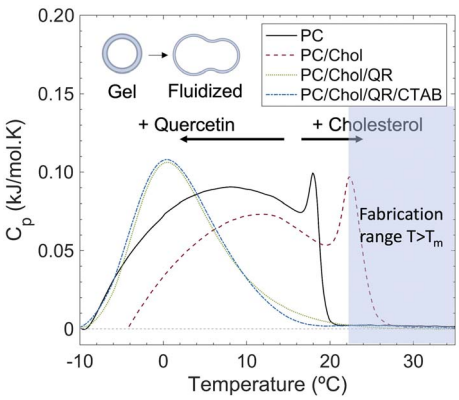

Fig. 2 Nano-DSC (differential scanning calorimetry) thermograms of liposomal suspensions upon the addition of cholesterol (Chol), model drug (quercetin, QR), and bioenhancer (CTAB). A unilamellar vesicle is shown as an example of fluidization of the membrane at the working temperatures used during preparation.

bioenhancer was encapsulated by liposomes without affecting their structural stability. The characterization of the T_m of modified and loaded liposomal suspensions is frequently absent in previous publications on the fabrication of complex materials for molecular release. In this work, these results are important as they confirm that the final liposomal suspensions were in a fluidized phase at room temperature, which will facilitate their fusion into the PCL fibers.

3.2 Parameter optimization for centrifugal spinning

The optimization of the parameters for centrifugal spinning is non-trivial and must be performed to maximize the fiber yield while minimizing the fiber diameter. Several polymers, concentrations, and solvent mixtures were tested for the centrifugal spinning.[29] However, only the combination of polycaprolactone and a 50 : 50 (v/v) methanol/chloroform solvent produced uniformly sized, small-diameter bead-free microfibers, as shown in Table S4.† The production of PCL fibers was performed using various spinning parameters: spinneret velocity (5000–9000 rpm) and spinning time (50–150 seconds). No fibers were produced below 5000 rpm within 50–150 seconds because these rotational speeds were insufficient to eject all the polymeric solution from the spinneret, resulting in no fiber formation. However, at 7000 rpm for 50 seconds, a low yield of fibers with many beads was produced. As the spinneret velocity increased to 8000 rpm, the fiber production rate increased. However, some beading of the fibers was still observed. By increasing the spinneret velocity to 9000 rpm for 50 seconds, bead-free microfibers with a uniform size distribution were obtained. This rotational speed resulted in continuous PCL microfibers. Thus, a spinneret velocity of 9000 rpm and a spinning time of 50 seconds were selected as optimal operating conditions for producing homogeneous forcespun PCL microfibers with uniform diameters.

3.3 SEM analysis of fibers before and after fusion with liposomes

Following microfiber production, the morphological and structural properties of forcespun PCL microfibers were examined using SEM analysis. SEM micrographs revealed that bead-free and homogeneous microfibers were produced at a PCL concentration of 20% (w/v), while large fiber sizes (>1 μm) with substantial bead formation were observed at a PCL concentration of 15% (w/v). The average fiber diameter for PCL (15%, w/v) was 1.413 ± 0.678 μm (Fig. S6†), while for PCL (20%, w/v), it was 584.85 ± 26.30 nm, as seen in Fig. 3a and b. SEM micrographs of the fused liposome/microfiber hybrids revealed that the coated liposomes were successfully loaded into the fibers or adsorbed on their surfaces. As shown in Fig. 3c and d, the hybrid materials were thicker, with rougher surfaces due to the incorporation of polymer-coated liposomes.

3.4 FT-IR analysis of liposomes and fibers

The FT-IR spectra of the liposomes and the hybrid fibers are shown in Fig. S4.† Peaks for QR were confirmed at 3406 and 3283 cm^{-1} (OH stretching) and 1379 cm^{-1} for the –OH bending

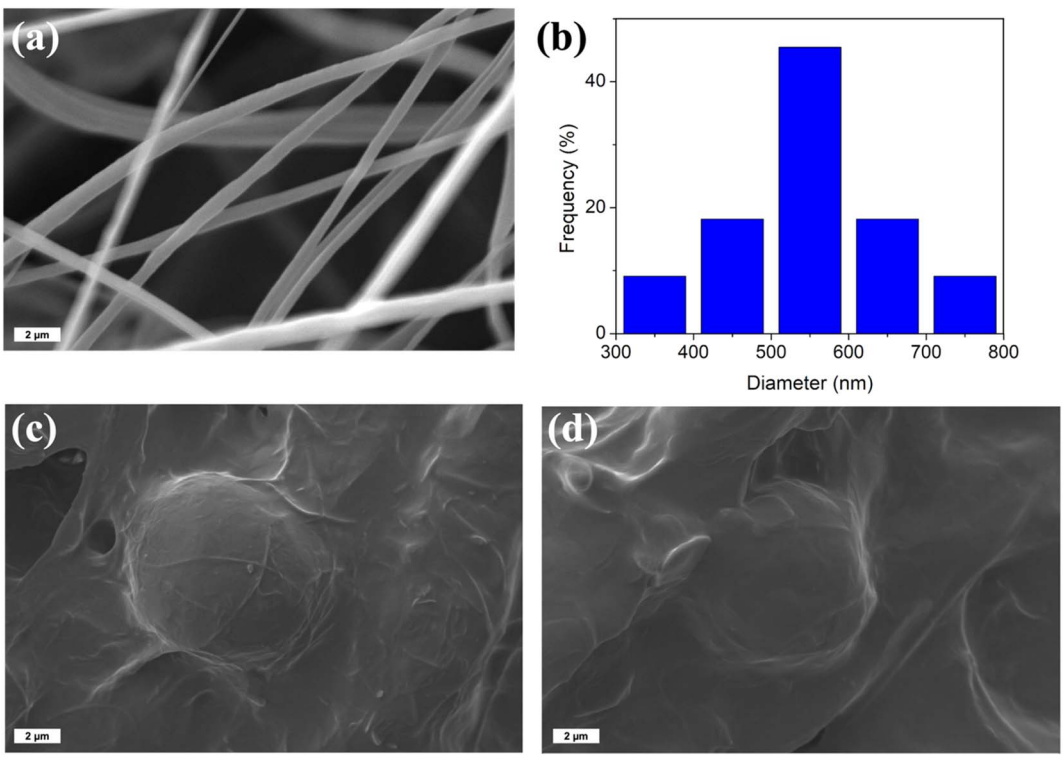

Fig. 3 Micrographic analysis of microfibers before and after fusion with the polymer-coated liposomes, (a) scanning electron micrographs (SEM) of plain PCL microfibers, (b) corresponding histogram of the fiber diameter, and (c and d) scanning electron micrographs (SEM) of the polymer-coated liposomes/microfibers hybrids showing effective fusion of the particles.

of the phenol group (Fig. S4d†). The C=O aryl ketonic stretch absorption was detectable at 1666 cm^{-1}. The C=C aromatic ring stretch bands were detectable at 1610, 1560, and 1510 cm^{-1}. The in-plane bending band of C–H in the aromatic hydrocarbon was detectable at 1317 cm^{-1}, and out-of-plane bending bands were detectable at 933, 820, and 600 cm^{-1}. The peaks at 1263, 1200, and 1165 cm^{-1} were assigned to the C–O stretching in the aryl ether ring, the C–O stretching in phenol, and the C–CO–C stretch and bending in ketone, respectively.[30] The characteristic peak in the FT-IR spectra of chitosan (Fig. S4c†) is 3447 cm^{-1}, which was attributed to NH_2 and OH groups stretching vibration. The peaks at 1657 and 1598 cm^{-1} were linked to the $CONH_2$ and NH_2 groups, respectively. The PEG absorption bands are shown in Fig. S4d:† 958 cm^{-1} and 2880 cm^{-1}, which were attributed to the C–H and CH_2 groups, respectively. The triplet at 1150 cm^{-1}, 1110 cm^{-1}, and 1060 cm^{-1} is assigned to the C–O–C groups.[31] The spectra of L-α-PC contain characteristic peaks at 2930 cm^{-1} (CH_2 stretching), 1737 cm^{-1} (C=O stretching), and 1461 cm^{-1} (C–H bending of CH_3), Fig. S4e.† Peaks at 3394 cm^{-1} (O–H stretching); 2930 cm^{-1} (CH_2 stretching); 1463 cm^{-1} (C–C aromatic stretching) and 1365 cm^{-1} (C–O stretching) were confirmed for cholesterol-containing samples. The FT-IR spectra of CTAB showed a characteristic peak at 3335 cm^{-1} for stretching vibrations of the ammonium group in CTAB. The peaks at 2930 cm^{-1} and 2854 cm^{-1} were attributable to two different C–H band vibrations of the CH_2 group in CTAB.[32] For the polymer-coated liposomes, the main functional peaks of chitosan and PEG-4000 were observed in the FT-IR spectra.

To identify the chemical interaction between liposomes and microfibers, the FT-IR spectra of QR- and CTAB-co-loaded liposomes and the fused liposome/microfiber constructs were compared, as shown in Fig. S4f.† The FT-IR spectra of PCL showed characteristic peaks at 2951 cm^{-1} and 2866 cm^{-1}, which were attributed to C–H stretching; 1725 cm^{-1}, which was attributed to C=O stretching vibration; and 1158 cm^{-1}, which was attributed to C–O–C stretching vibration. There was no difference in PCL in the solid and fiber states. The main functional peaks of plain liposomes, chitosan, PEG-4000, and PCL were observed in the FT-IR spectra of the hybrid materials.

3.5 Thermal analysis of the fibers before and after addition of liposomes

Thermal gravimetric analysis (TGA) was used to measure the thermal stability and decomposition behavior of the liposome/microfiber hybrids as compared to that of the PCL microfibers, shown in Fig. 4. The plain microfibers showed thermal decomposition in the temperature range of 350–470 °C. They showed an initial degradation temperature ($T_{(0.1)}$) of around 360 °C and a midpoint degradation temperature ($T_{(0.5)}$) at 460 °C. In contrast, the hybrid fibers containing chitosan show thermal decomposition in the 240–420 °C range, with $T_{(0.1)}$ around 250 °C and $T_{(0.5)}$ at 400 °C. The PEG-containing fiber hybrids have a thermal decomposition in the 240–480 °C range, with $T_{(0.1)}$ ~250 °C and $T_{(0.5)}$ at 450 °C. The thermal degradation of PCL was accelerated upon the addition of the polymer

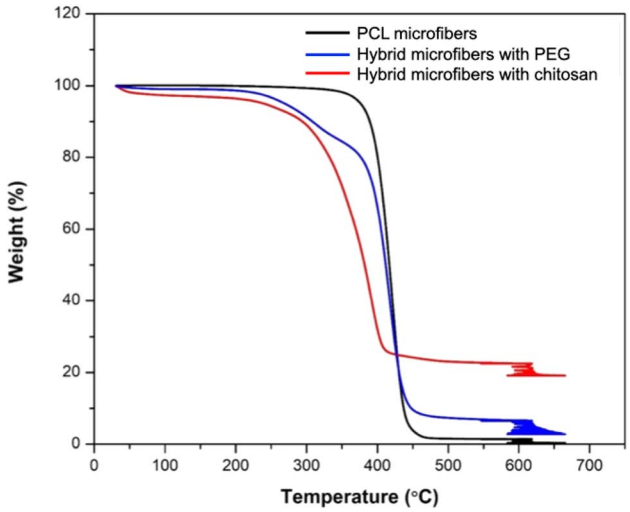

Fig. 4 TGA curves of plain fibers against the chitosan and polyethylene glycol (PEG) containing hybrid materials.

coatings, being lower than that of the hybrids with chitosan-coated or PEG-coated liposomes (Fig. S5†). The melting point of PCL occurs at around 55–60 °C, whereas the melting of PC occurs at around 54 °C. The melting temperature of chitosan ranges from around 102 to 220 °C, depending on multiple variables including purity and molecular weight. On the other hand, the melting point of PEG-4000 ranges around 50–60 °C. The main point of the TGA analysis is to provide additional evidence of the blending of polymers and liposomes. The variation in melting temperatures may influence the observed changes in the thermograms. However, the results support that the polymer-coated liposomes are blending with the PCL fibers.

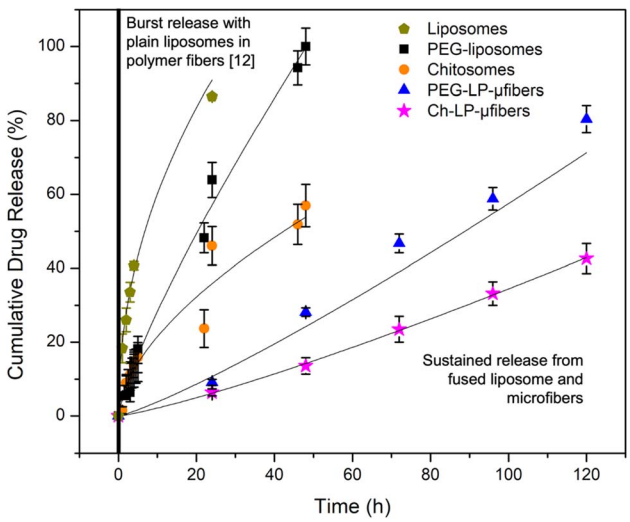

Fig. 5 Drug release profiles of the polymer-coated liposomes/microfiber hybrids against the release from the polymer-coated liposomes and referenced to the burst release reported for plain liposomes in fibers. Solid lines show the fitting to the Korsmeyer–Peppas kinetic model.

Table 1 Drug release rate parameters of the Korsmeyer–Peppas kinetic model for LP–QR–CTAB–CH–NF and LP–QR–CTAB–PEG–NF hybrid materials[a]

Formula code	Linear fit	R^2	K	SSD	n
LP–QR–CTAB–CH–NF	$y = 1.19x - 0.85$	0.999	0.134	0.806	1.205
LP–QR–CTAB–PEG–NF	$y = 1.33x - 0.84$	0.994	25.338	105.248	1.178

[a] Coefficient of determination (R^2); rate constant (K); sum of the squared difference (SSD); release exponent (n). $n \leq 0.45$: Fickian diffusion (case-I transport); $0.45 < n < 0.89$: anomalous (non-Fickian) diffusion; $n \simeq 0.89$: zero-order release (case-II transport); $n > 0.89$: super case-II transport.

3.6 Molecular release kinetic studies

The release of QR from the polymer-coated liposomes at physiological pH 7.4 is illustrated in Fig. S3b.† Both liposomal systems show stable release profiles without an initial burst release. After 48 hours of drug release, the cumulative drug release was 59.96 ± 5.74% with chitosan coating *versus* 99.84 ± 4.98% with PEG coating. The release of the molecular cargo may be affected by dissolution, diffusion, swelling, erosion, and degradation.[33] To understand the drug release kinetics of polymer-coated liposomes, the drug release profiles were fitted against five mathematical models, Table S5, Fig. S6 and S7.† The chitosan-coated liposomes were found to follow the Higuchi release with an $R^2 = 0.968$, indicating a diffusion-driven controlled drug mechanism. In turn, the PEG-coated liposomes follow zero-order release with an $R^2 = 0.9857$, owing to the presence of the PEG coating on the liposomal surface, which resulted in more sustained action.[34]

To further understand the drug release mechanisms of polymer-coated liposomes, drug release data were analyzed using the Korsmeyer–Peppas kinetic model (Table S6†). The chitosan-coated liposomes yielded a release equation where $n = 0.585$, $K = 5.587$, and $R^2 = 0.930$, indicating that the release mechanism follows anomalous (non-Fickian) diffusion, which is a combination of both diffusion and erosion mechanisms. In contrast, the equation for the release with the PEG-coated liposomes follows $n = 0.802$, $K = 4.465$, and $R^2 = 0.981$, indicating that the release mechanism is near-zero-order release (case-II transport), implying that the drug is released primarily through swelling and erosion mechanisms. Thus, the PEG-coated liposome showed a better controlled release profile than the chitosan-coated liposome, as ideal controlled release systems frequently aim for zero-order release.[35]

The drug release from the liposome/microfiber hybrids was evaluated in PBS of pH 7.2 at 37 °C. Both hybrid materials showed lower drug release rates as compared to the coated liposomes alone, which is expected from the additional diffusional barrier. Notably, the liposome/microfiber hybrids displayed a gradual and prolonged drug release for 120 hours. The total amount of QR released after 120 hours of drug release was 42.656 ± 4.07% for the hybrid material with chitosan and 80.405 ± 3.67% for the hybrid material with PEG (Fig. 5).

To understand the drug release kinetics of liposome/microfiber hybrids, data obtained from drug release testing were analyzed using zero-order release kinetics, the Higuchi square release model, and the Korsmeyer–Peppas kinetic model. The hybrid materials follow zero-order release, with R^2 values equal to 0.9966 and 0.9954 for chitosan- and PEG- containing hybrids, respectively. The release from the chitosan-containing hybrid follows $n = 1.205$, $K = 0.134$, and $R^2 = 0.999$, indicating that the release mechanism is a pure super case-II transport mechanism due to the erosion of the polymeric fibrous structure.[36] Similarly, the release from the PEG-containing hybrid was fitted to $n = 1.178$, $K = 0.284$, and $R^2 = 0.994$, indicating that the release mechanism is also a pure super case-II transport mechanism in which the drug release from the hybrid is controlled by the erosion of the polymeric fibrous structure (Table 1).[37,38] Overall, the PEG-coated liposome exhibited a near-zero-order controlled release, whereas the PEG-containing hybrids follow Higuchi release. The addition of the liposomes into the microfibers increased controlled release characteristics, resulting in zero-order release profiles and a super case-II transport mechanism.

4 Conclusion

Hybrid materials were fabricated from the fusion of polymer-coated liposomes with polycaprolactone microfibers to enhance the sustained release of molecular cargo. Fibers were produced by centrifugal spinning and liposomes integrated by immersion under sonication. The critical parameters for producing uniform bead-free fibers were adjusted to a PCL concentration of 20% (w/v) in a 50 : 50 (v/v) solvent mixture of methanol and chloroform. The average fiber diameter was 584.85 ± 26.30 nm, which was adequate for loading the coated liposomes. Nano-DSC and SEM support that liposomes were adequate to fuse into the microfibrous scaffold. The total amount of QR released after 120 hours of drug release was 42.656 ± 4.07% and 80.405 ± 3.67% for the chitosan- and PEG-containing hybrid materials, respectively. Their release mechanism is a pure super case-II transport mechanism in which the drug release from the hybrid materials is controlled by the erosion and swelling of the polymeric microfibers. These findings demonstrate that liposome/microfiber hybrid materials produced through a scalable process can outperform plain liposomes in terms of stability and sustained release.

Data availability

The data supporting this article have been included as part of the ESI.†

Conflicts of interest

The authors declare no conflict of interest.

Acknowledgements

This project was partially financed by the Consejo Nacional de Humanidades, Ciencias, y Tecnología (CONAHCYT), grant application number 2022-000018-02NACF-14173 for Ahmed M. Agiba and by Tecnologico de Monterrey through the Challenge-Based Research Funding Program 2022 (Project ID IJXT070-22EG57001) for Omar Lozano and Alan Aguirre-Soto. Francisco J. Sierra-Valdez acknowledges financial support provided by the Federico Baur Endowed Research Chair in Nanotechnology (0020206BA1).

References

1 R. R. Sawant and V. P. Torchilin, Liposomes as 'smart' pharmaceutical nanocarriers, *Soft Matter*, 2010, **6**, 4026–4044.
2 I. Hasan, *et al.*, A state-of-the-art liposome technology for glioblastoma treatment, *Nanoscale*, 2023, **15**, 18108–18138.
3 N. Aminu, *et al.*, Applications of nanofibers drug delivery system in cancer therapy, *J. Drug Delivery Sci. Technol.*, 2023, 105128.
4 J. Chen, *et al.*, Review of the principles, devices, parameters, and applications for centrifugal electrospinning, *Macromol. Mater. Eng.*, 2022, **307**, 2200057.
5 K. Sarkar, *et al.*, Electrospinning to forcespinning™, *Mater. Today*, 2010, **13**, 12–14.
6 N. Mamidi, H. M. L. Gutiérrez, J. Villela-Castrejón, L. Isenhart, E. V. Barrera and A. Elías-Zúñiga, Fabrication of gelatin-poly (epichlorohydrin-co-ethylene oxide) fiber scaffolds by Forcespinning® for tissue engineering and drug release, *MRS Commun.*, 2017, **7**, 913–921.
7 N. Mamidi, I. L. Romo, E. V. Barrera and A. Elías-Zúñiga, High throughput fabrication of curcumin embedded gelatin-polylactic acid forcespun fiber-aligned scaffolds for the controlled release of curcumin, *MRS Commun.*, 2018, **8**, 1395–1403.
8 K. Hasanbegloo, *et al.*, Paclitaxel-loaded liposome-incorporated chitosan (core)/poly (ε-caprolactone)/chitosan (shell) nanofibers for the treatment of breast cancer, *Int. J. Biol. Macromol.*, 2023, **230**, 123380.
9 C. Tantisripreecha, M. Jaturanpinyo, B. Panyarachun and N. Sarisuta, Development of delayed-release proliposomes tablets for oral protein drug delivery, *Drug Dev. Ind. Pharm.*, 2012, **38**, 718–727.
10 R. Li, *et al.*, Liposomes coated with thiolated chitosan as drug carriers of curcumin, *Mater. Sci. Eng., C*, 2017, **80**, 156–164.
11 S. Gopi, A. Amalraj, J. Jacob, N. Kalarikkal, S. Thomas and Q. Guo, Preparation, characterization and in vitro study of liposomal curcumin powder by cost effective nanofiber weaving technology, *New J. Chem.*, 2018, **42**, 5117–5127.
12 M. Rampichová, *et al.*, Functionalization of 3D fibrous scaffolds prepared using centrifugal spinning with liposomes as a simple drug delivery system, *Acta Polytech. CTU Proc.*, 2017, **8**, 24–26.
13 O. Lozano, D. Solis-Castañol, S. Cantú-Casas, P. I. M. Muraira and G. García-Rivas, A review of quercetin delivery through nanovectors: cellular and mitochondrial effects on noncommunicable diseases, *Mol. Nutr. Mitochondria*, 2023, pp. 363–382.
14 X. Chen, O. Q. P. Yin, Z. Zuo and M. S. S. Chow, Pharmacokinetic modeling of quercetin and metabolites, *Pharm. Res.*, 2005, **22**, 892–901.
15 G. M. Demirbolat, Ö. Erdoğan, G. P. Coşkun and Ö. Çevik, PEG4000 modified liposomes enhance the solubility of quercetin and improve the liposome functionality: in vitro characterization and the cellular efficacy, *Turk. J. Chem.*, 2022, **46**, 1011–1023.
16 C. Has and P. Sunthar, A comprehensive review on recent preparation techniques of liposomes, *J. Liposome Res.*, 2020, **30**(4), 336–365.
17 J. Thongborisute, H. Takeuchi, H. Yamamoto and Y. Kawashima, Visualization of the penetrative and mucoadhesive properties of chitosan and chitosan-coated liposomes through the rat intestine, *J. Liposome Res.*, 2006, **16**, 127–141.
18 J. Li, *et al.*, Effect of a drug delivery system made of quercetin formulated into PEGylation liposomes on cervical carcinoma in vitro and in vivo, *J. Nanomater.*, 2021, **2021**, 1–12.
19 N. Mamidi, A. E. Zuníga and J. Villela-Castrejón, Engineering and evaluation of forcespun functionalized carbon nano-onions reinforced poly (ε-caprolactone) composite nanofibers for pH-responsive drug release, *Mater. Sci. Eng., C*, 2020, **112**, 110928.
20 R. Jangde and D. Singh, Preparation and optimization of quercetin-loaded liposomes for wound healing, using response surface methodology, *Artif. Cells, Nanomed., Biotechnol.*, 2016, **44**, 635–641.
21 S. Jagwani, S. Jalalpure, D. Dhamecha, K. Jadhav and R. Bohara, Pharmacokinetic and pharmacodynamic evaluation of resveratrol loaded cationic liposomes for targeting hepatocellular carcinoma, *ACS Biomater. Sci. Eng.*, 2020, **6**, 4969–4984.
22 J. Sun, Y. Song, M. Lu, X. Lin, Y. Liu, S. Zhou, Y. Su and Y. Deng, Evaluation of the antitumor effect of dexamethasone palmitate and doxorubicin co-loaded liposomes modified with a sialic acid–octadecylamine conjugate, *Eur. J. Pharm. Sci.*, 2016, **93**, 177–183.
23 R. Huang and C. Xu, An overview of the perception and mitigation of astringency associated with phenolic compounds, *Compr. Rev. Food Sci. Food Saf.*, 2021, **20**, 1036–1074.
24 T. Kaasgaard and T. L. Andresen, Liposomal cancer therapy: exploiting tumor characteristics, *Expert Opin. Drug Delivery*, 2010, **7**, 225–243.
25 N. Berger, A. Sachse, J. Bender, R. Schubert and M. Brandl, Filter extrusion of liposomes using different devices: comparison of liposome size, encapsulation efficiency, and process characteristics, *Int. J. Pharm.*, 2001, **223**, 55–68.
26 A. Panya, M. Laguerre, J. Lecomte, P. Villeneuve, J. Weiss, D. J. McClements and E. A. Decker, Effects of chitosan and

rosmarinate esters on the physical and oxidative stability of liposomes, *J. Agric. Food Chem.*, 2010, **58**, 5679–5684.

27 J. M. Bezemer, R. Radersma, D. W. Grijpma, P. J. Dijkstra, J. Feijen and C. A. Van Blitterswijk, Zero-order release of lysozyme from poly (ethylene glycol)/poly (butylene terephthalate) matrices, *J. Controlled Release*, 2000, **64**, 179–192.

28 D. Needham, Cohesion and permeability of lipid bilayer vesicles, in *Permeability and Stability of Lipid Bilayers*, CRC Press, 2017, pp. 49–76.

29 L. M. Dominak and C. D. Keating, Polymer encapsulation within giant lipid vesicles, *Langmuir*, 2007, **23**, 7148–7154.

30 M. Catauro, F. Papale, F. Bollino, S. Piccolella, S. Marciano, P. Nocera and S. Pacifico, Silica/quercetin sol-gel hybrids as antioxidant dental implant materials, *Sci. Technol. Adv. Mater.*, 2015, **16**, 035001.

31 C. Lustriane, F. M. Dwivany, V. Suendo and M. Reza, Effect of chitosan and chitosan-nanoparticles on post-harvest quality of banana fruits, *J. Plant Biotechnol.*, 2018, **45**, 36–44.

32 R. S. Nair, N. Billa, L. Y. Mooi and A. P. Morris, Characterization and ex vivo evaluation of curcumin nanoethosomes for melanoma treatment, *Pharm. Dev. Technol.*, 2022, **27**, 72–82.

33 J. Di, X. Gao, Y. Du, H. Zhang, J. Gao and A. Zheng, Size, shape, charge and "stealthy" surface: carrier properties affect the drug circulation time in vivo, *Asian J. Pharm. Sci.*, 2021, **16**, 444–458.

34 R. Gupta, Y. Chen and H. Xie, In vitro dissolution considerations associated with nano drug delivery systems, *Wiley Interdiscip. Rev.:Nanomed. Nanobiotechnol.*, 2021, **13**, e1732.

35 P. Panwar, B. Pandey, P. C. Lakhera and K. P. Singh, Preparation, characterization, and in vitro release study of albendazole-encapsulated nanosize liposomes, *Int. J. Nanomed.*, 2010, **5**, 101–108.

36 I. F. Tannock and D. Rotin, Acid pH in tumors and its potential for therapeutic exploitation, *Cancer Res.*, 1989, **49**, 4373–4384.

37 A. M. Moydeen, M. S. Ali Padusha, E. F. Aboelfetoh, S. S. Al-Deyab and M. H. El-Newehy, Fabrication of electrospun poly(vinyl alcohol)/dextran nanofibers via emulsion process as drug delivery system: kinetics and in vitro release study, *Int. J. Biol. Macromol.*, 2018, **116**, 1250–1259.

38 Q.-Z. Zhai, Inclusion of cefalexin in SBA-15 mesoporus material and release property, *Mater. Sci. Eng., C*, 2012, **32**, 2411–2417.